Single-crystal diamond pixelated radiation detector with buried graphitic electrodes

C. Bloomer [1,2]
L. Bobb [1]
M. Newton [2]

[1] Diamond Light Source Ltd, Didcot, UK
[2] University of Warwick, Coventry, UK

Outline

- Motivation
- Introduction to diamond detectors
- Laser processing of diamond review
- Detector design and readout method
- First results and beam images
- Conclusions

Motivation

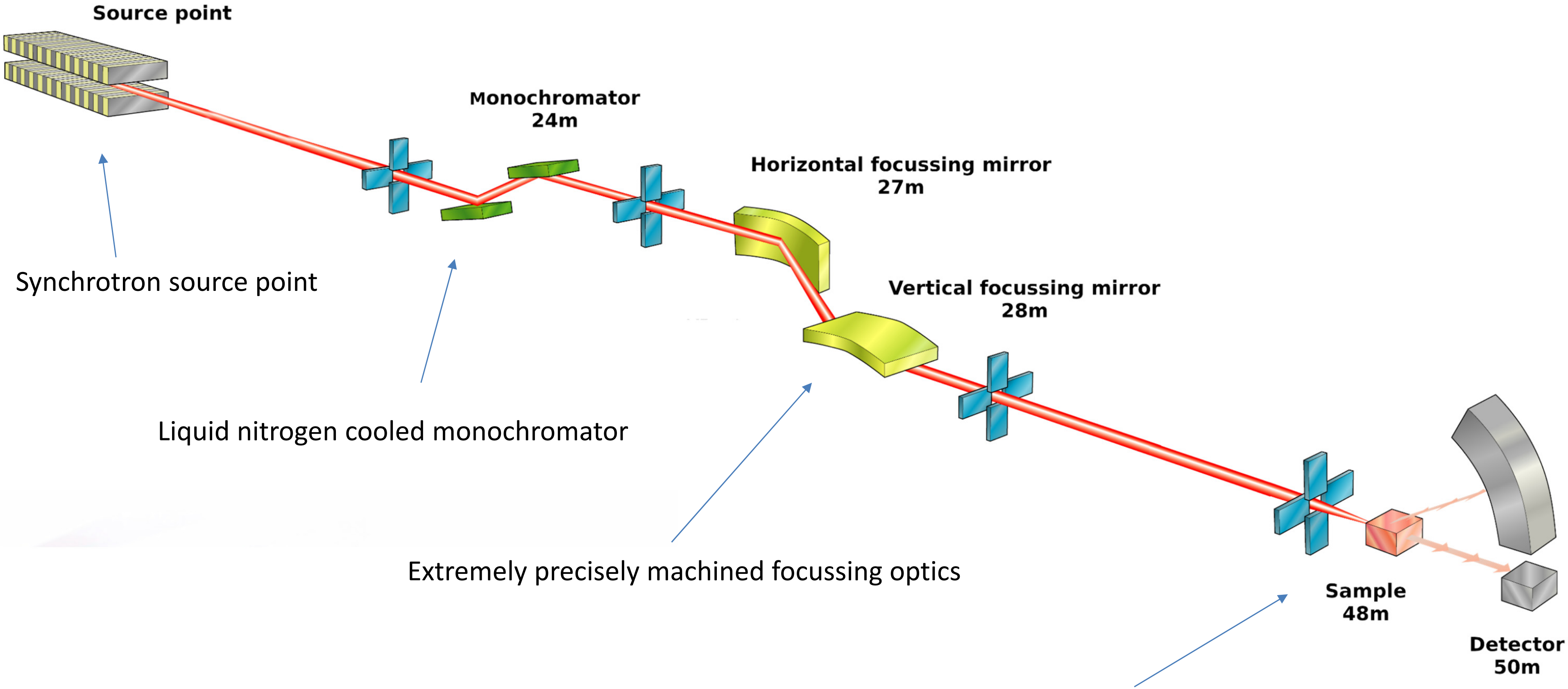

Synchrotron source point

Liquid nitrogen cooled monochromator

Extremely precisely machined focussing optics

1µm X-ray beams at the sample point

Motivation

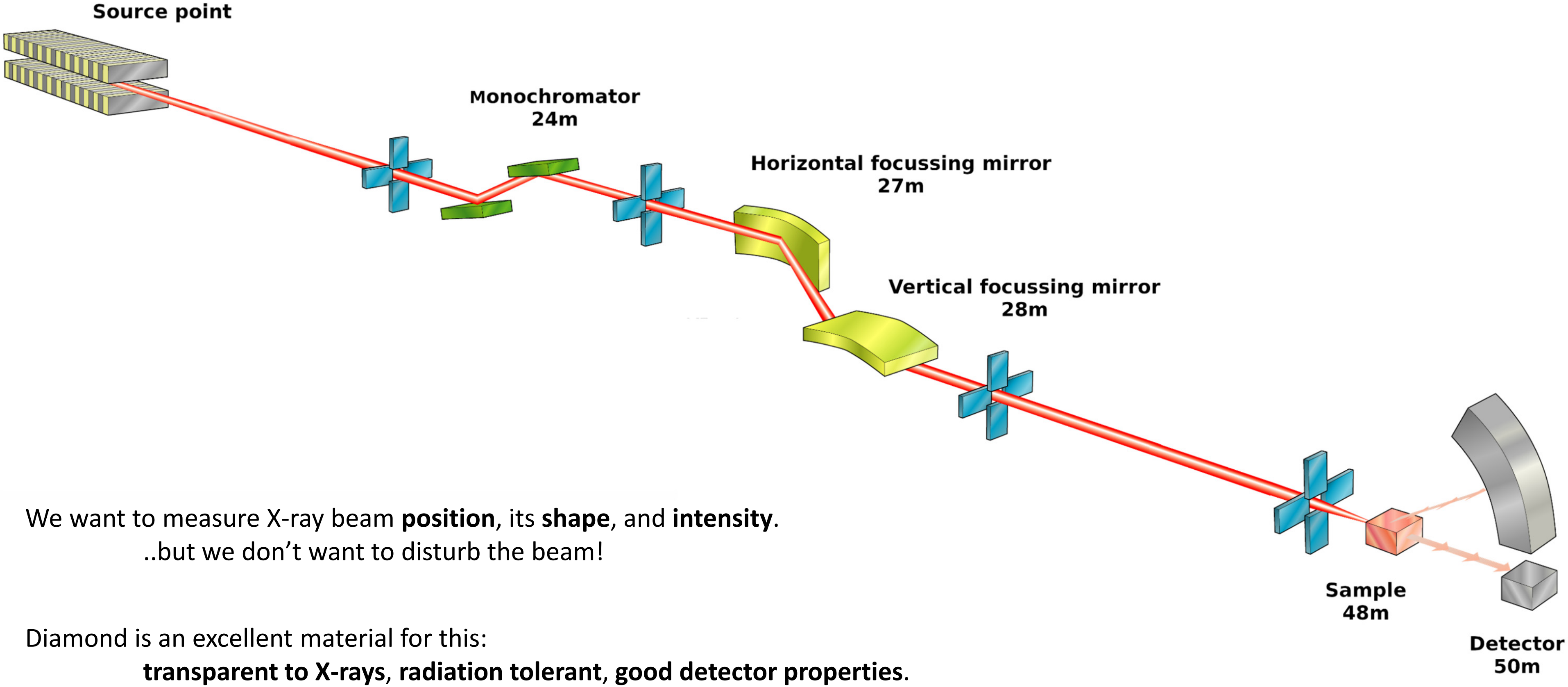

We want to measure X-ray beam **position**, its **shape**, and **intensity**.
..but we don't want to disturb the beam!

Diamond is an excellent material for this:
transparent to X-rays, **radiation tolerant**, **good detector properties**.

Diamond detectors

Diamond X-ray transmission compared to other detector materials

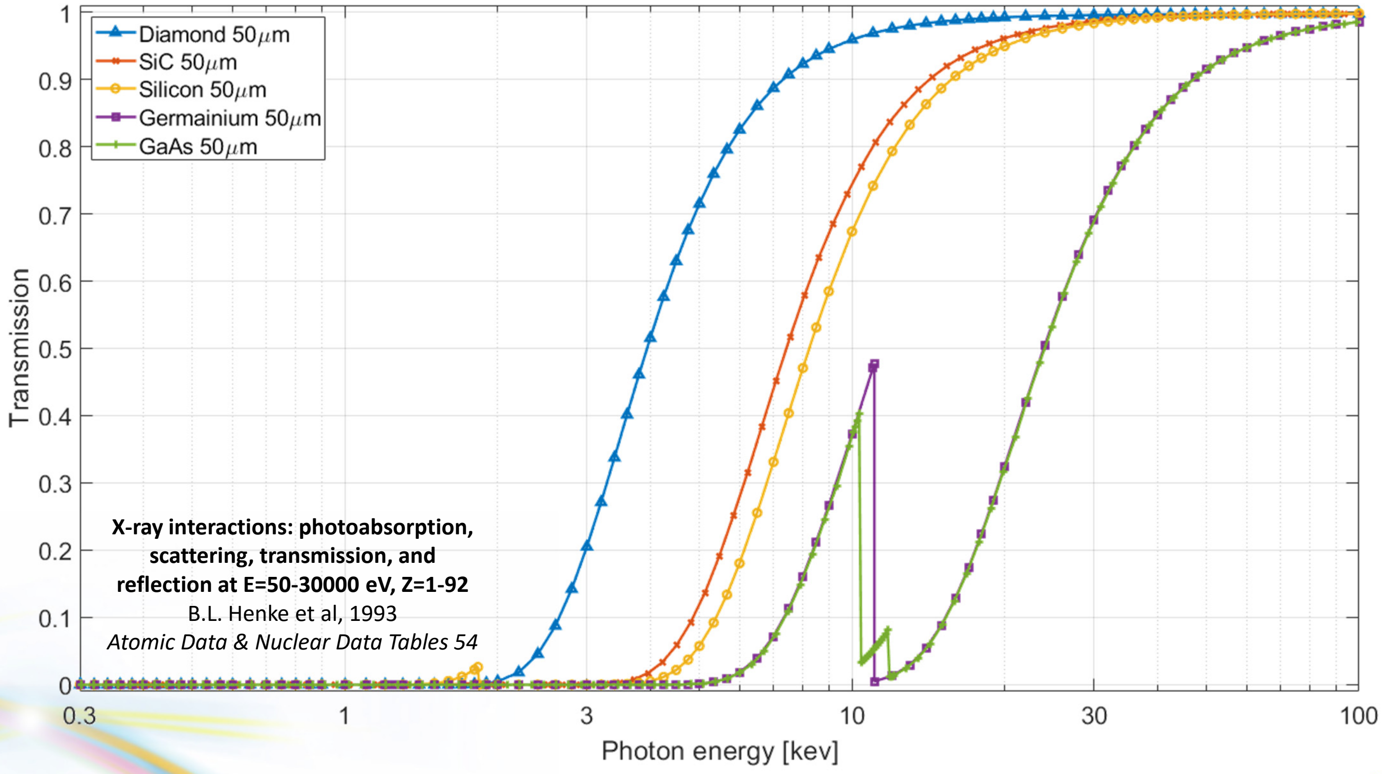

X-ray interactions: photoabsorption, scattering, transmission, and reflection at E=50-30000 eV, Z=1-92
B.L. Henke et al, 1993
Atomic Data & Nuclear Data Tables 54

Diamond detectors

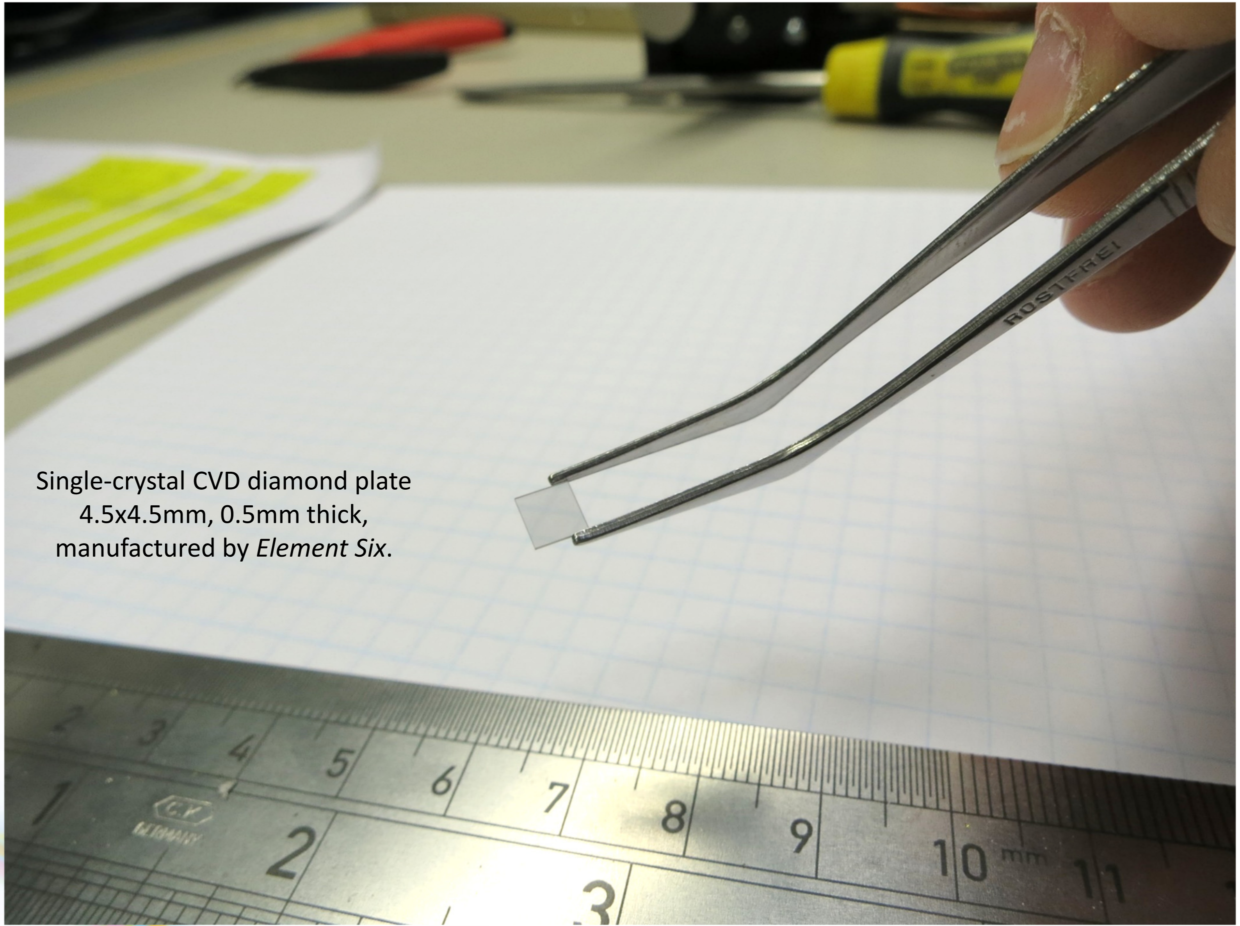
Single-crystal CVD diamond plate
4.5x4.5mm, 0.5mm thick,
manufactured by *Element Six*.

Diamond detectors

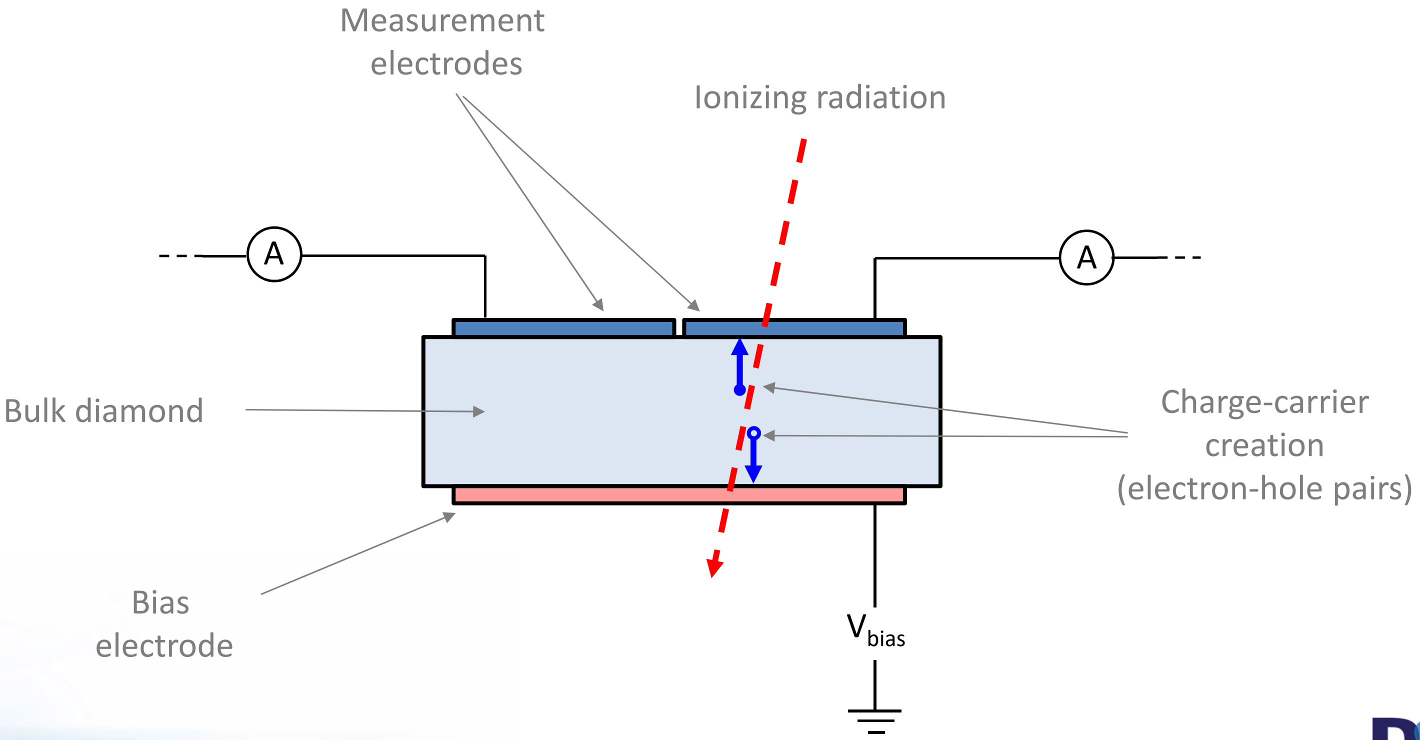

Measurement electrodes

Ionizing radiation

Bulk diamond

Charge-carrier creation (electron-hole pairs)

Bias electrode

Diamond detectors

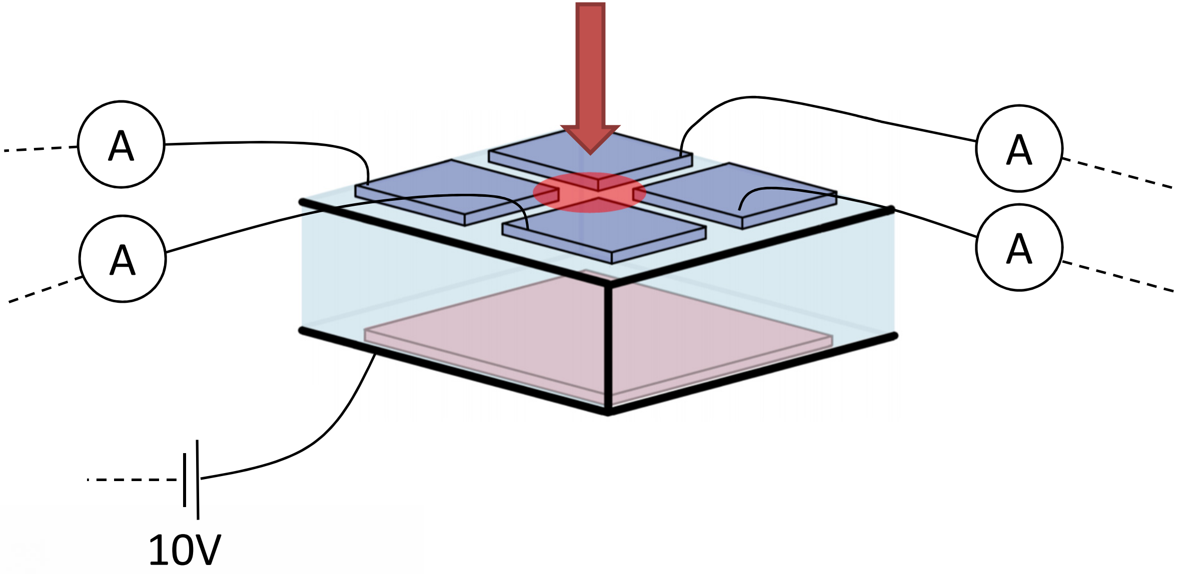

Problems with surface metallisation

..radiation damage
..ozone degradation
..mechanical damage

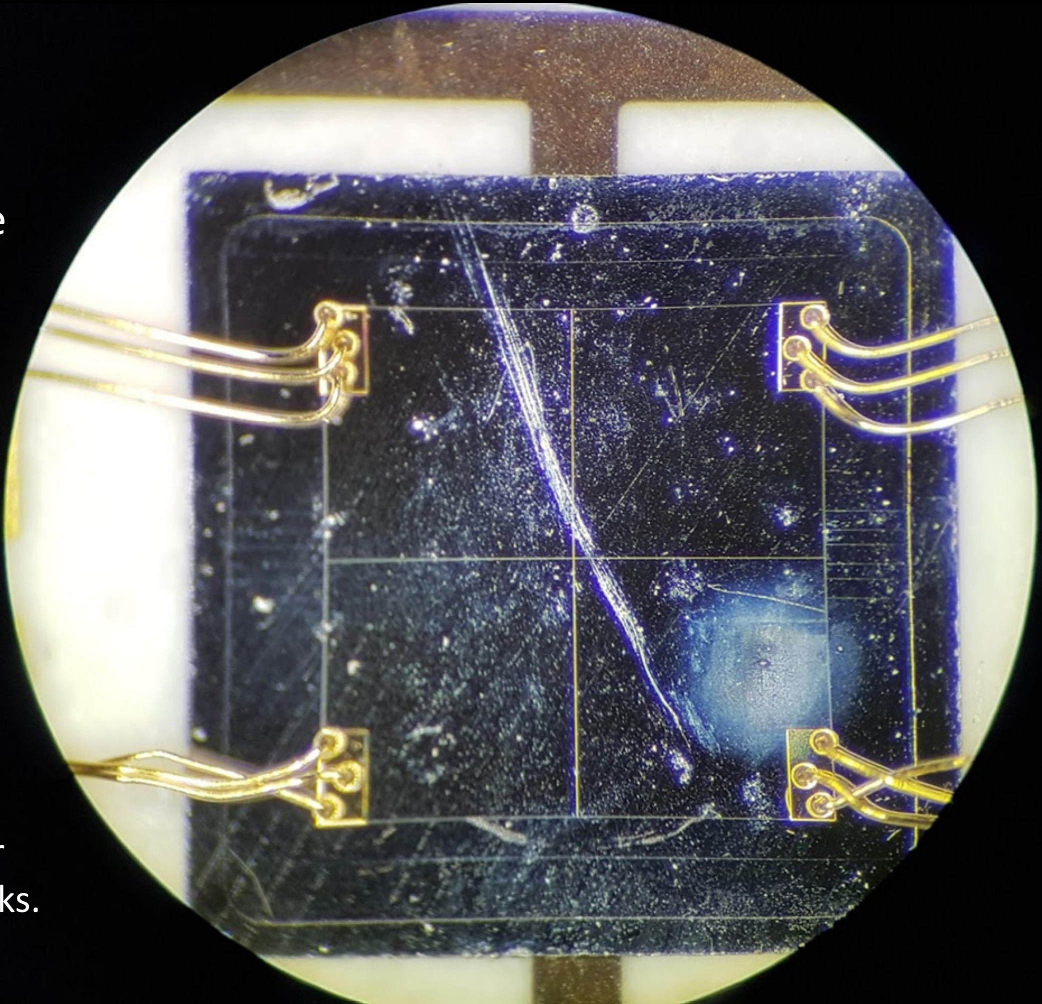

Detector taken from one of Diamond’s beamlines after accidental use in air with high flux for ~2 weeks.

Problems with surface metallisation

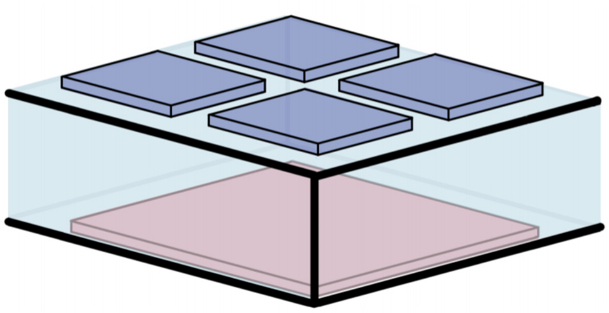

…bury the electrodes?

Laser processing of diamond

Conductive wires produced within bulk diamond using laser pulses.

Formation of buried p-type conducting layers in diamond

R. Walker et al, 1997
Appl. Phys. Lett. 71

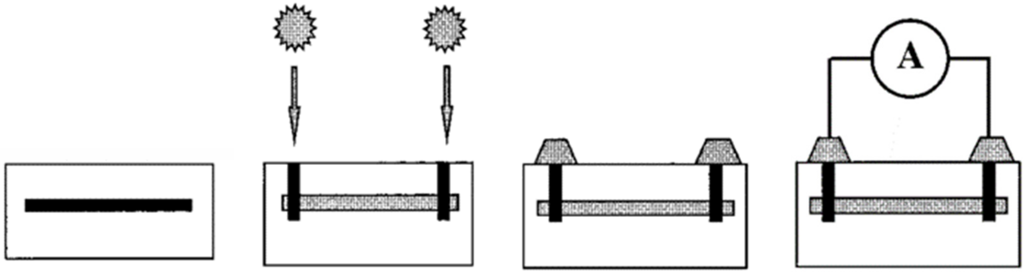

Laser processing of diamond

Conductive wires produced within bulk diamond using laser pulses.
~200fs long, **~50nJ per pulse**, focused down to **~1um in size**.

A novel detector with graphitic electrodes in CVD diamond
A. Oh *et al*, 2013
Diamond & Related Materials 38

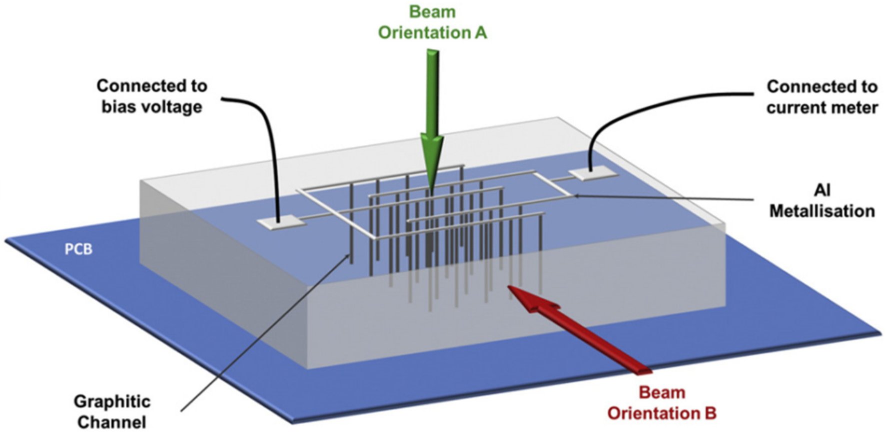

A 3D diamond detector for particle tracking
F. Bachmair *et al*, 2015
Nucl. Inst. Met. A 786

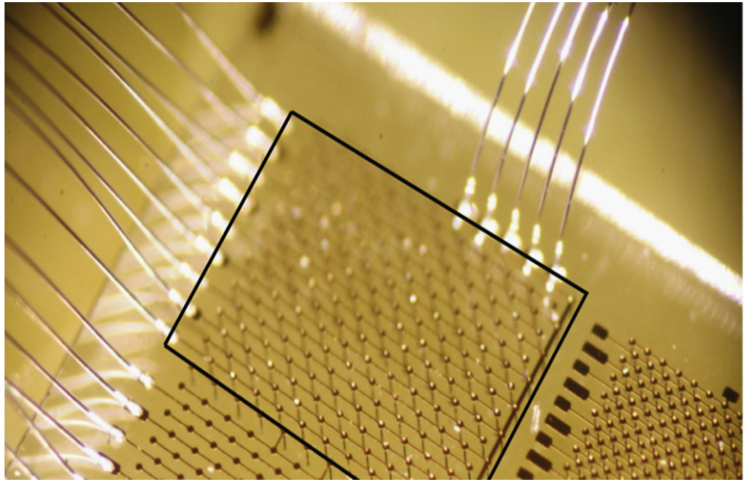

Laser processing of diamond

Conductive wires produced within bulk diamond using laser pulses.

~200fs long, **~50nJ per pulse**, focused down to **~1um in size**.

Adaptive optics allow effective focus at varying depths within the material.

High conductivity micro-wires in diamond following arbitrary paths

B. Sun *et al*, 2014
Appl. Phys. Lett 105

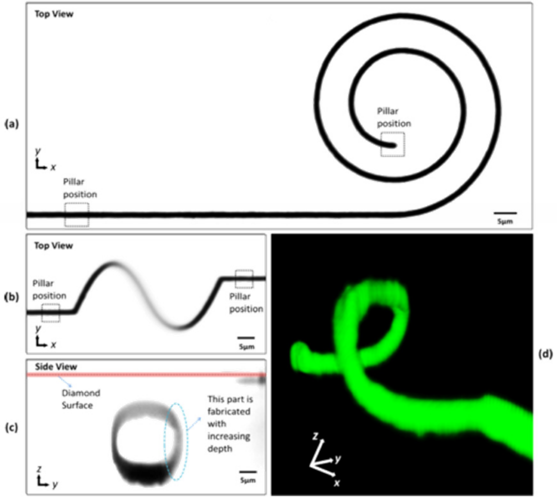

Very long laser-induced graphitic pillars buried in single-crystal CVD- diamond for 3D detectors realization

A. Khomich *et al*, 2018
Diamond & Related Materials 90

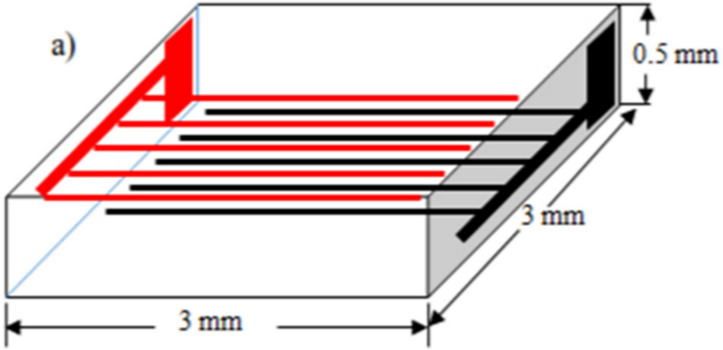

Laser processing of diamond

Conductive wires produced within bulk diamond using laser pulses.

~200fs long, **~50nJ per pulse**, focused down to **~1um in size**.

Adaptive optics allow effective focus at varying depths within the material.

Diamond photonics platform enabled by femtosecond laser writing

B. Sotillo *et al*, 2016
Nature Scientific Reports 6

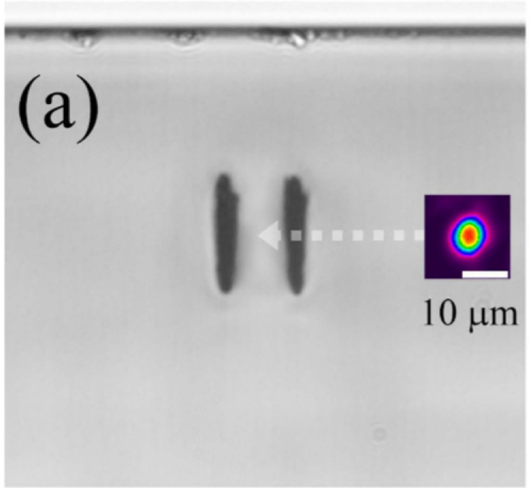

Laser writing of coherent colour centres in diamond

Y-C. Chen *et al*, 2016
Nature Photonics 11

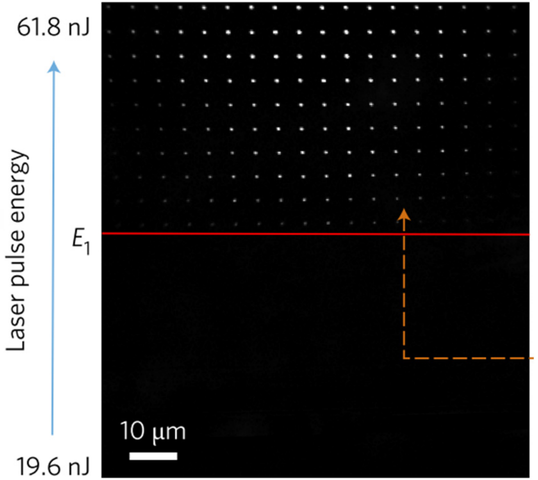

OPSYDIA

https://opsydia.com/, Formed 2017

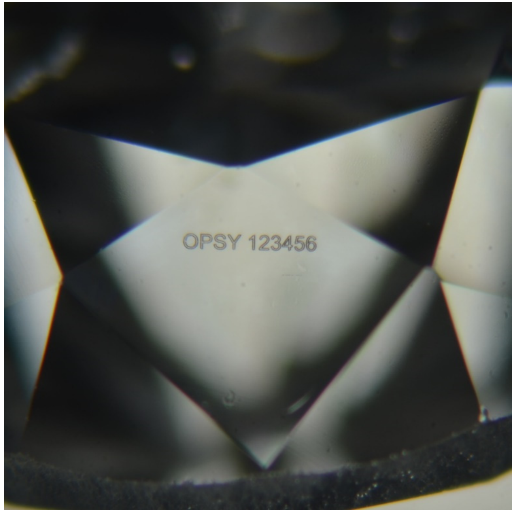

Diamond pixel detector

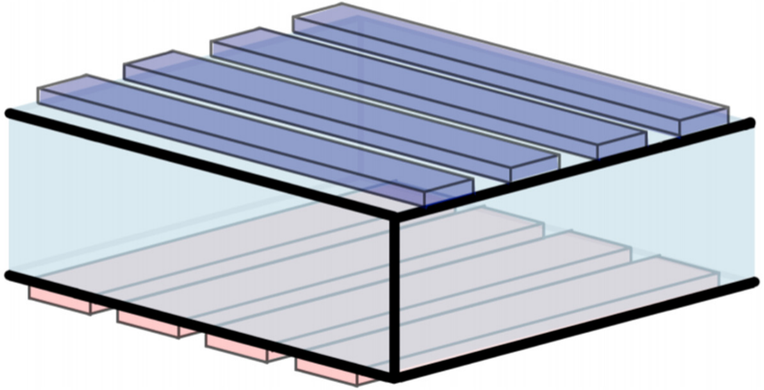

Pixelated transmission-mode diamond X-ray detector

T. Zhou *et al*, 2015

J. Synchrotron Radiation 22

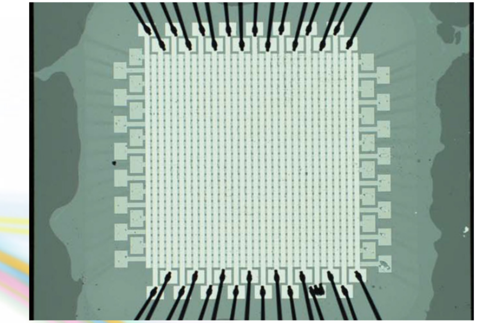

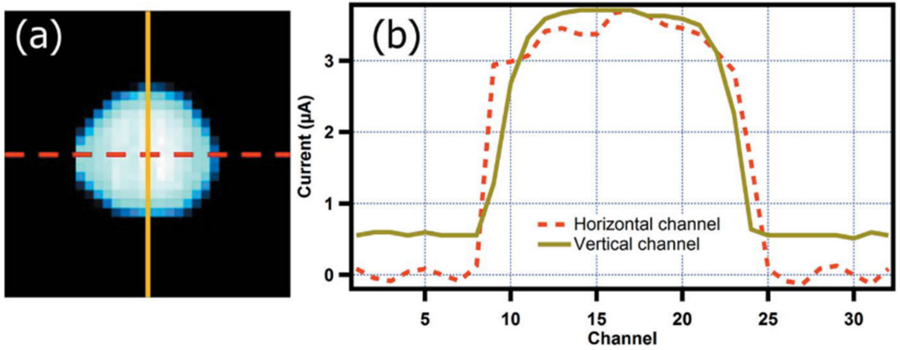

Graphitic-wire pixel detector

Pixel rows read-out **asynchronously**.

Around **~30fps** achieved using this technique by Zhou *et al.*

Limited by how quickly bias can be cleanly switched from electrode-to-electrode.

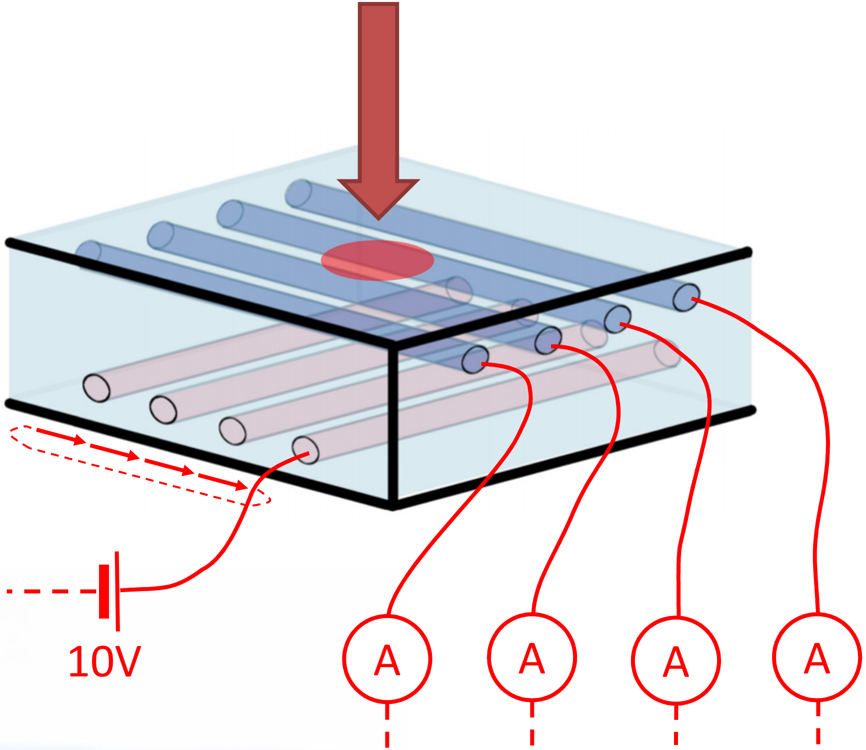

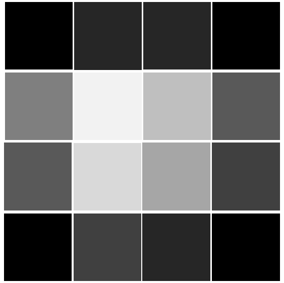

C Bloomer, IBIC 2021

Graphitic-wire pixel detector

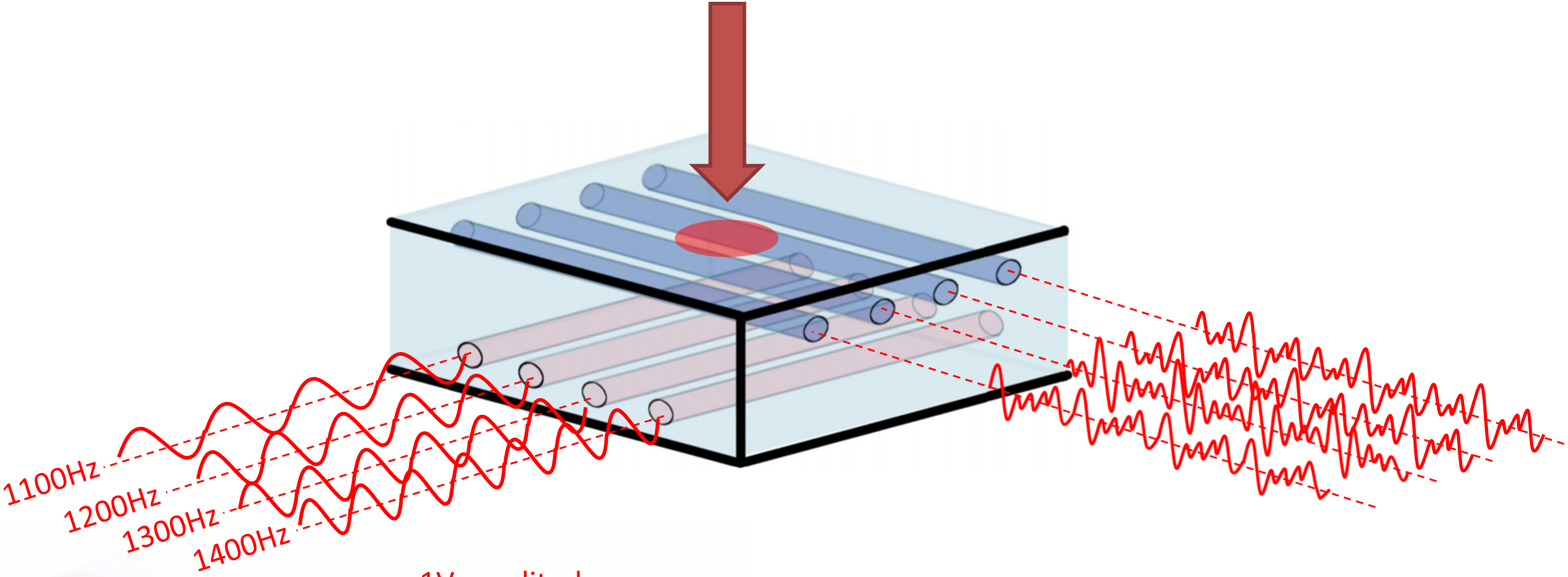

1V amplitude

Graphitic-wire pixel detector

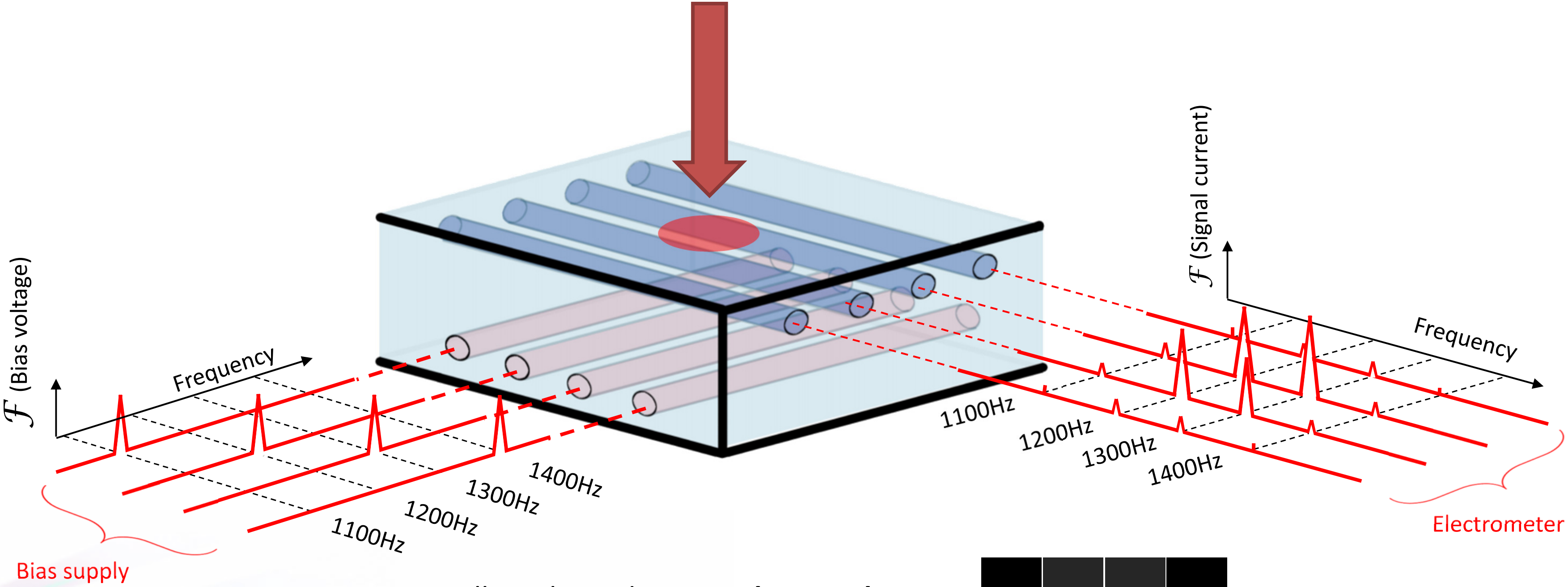

All pixels read out **synchronously**.

100fps achieved using this technique! Only limited by the relatively poor DAC speed we had available.

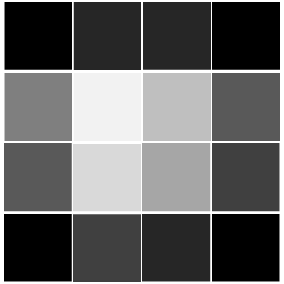

Fabrication

Element Six
'Single Crystal
Optical Plus'
grade material.

Laser-writing of wires:
Patrick Salter
(U. Oxford)

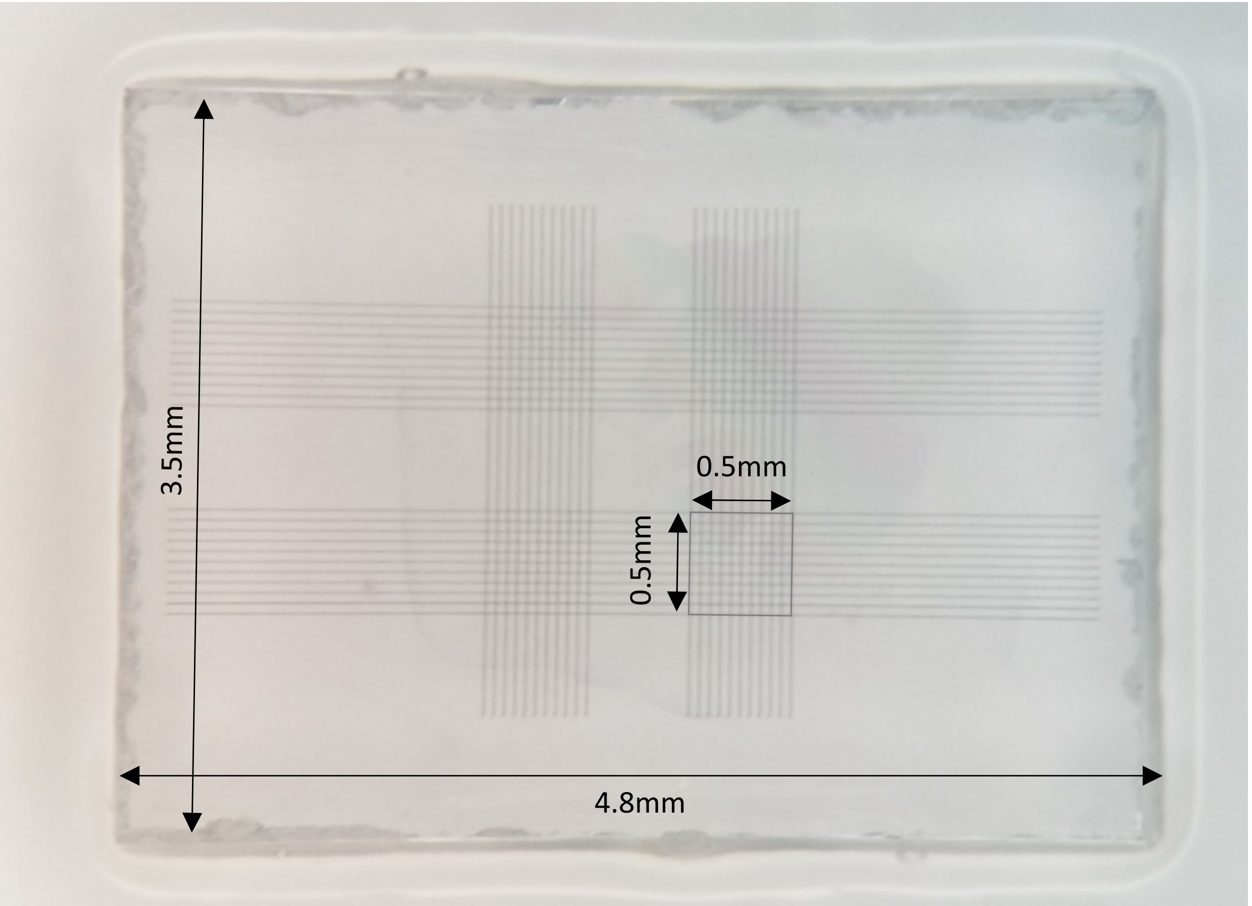

Fabrication

Metallisation:
Ben Green
(U. Warwick)

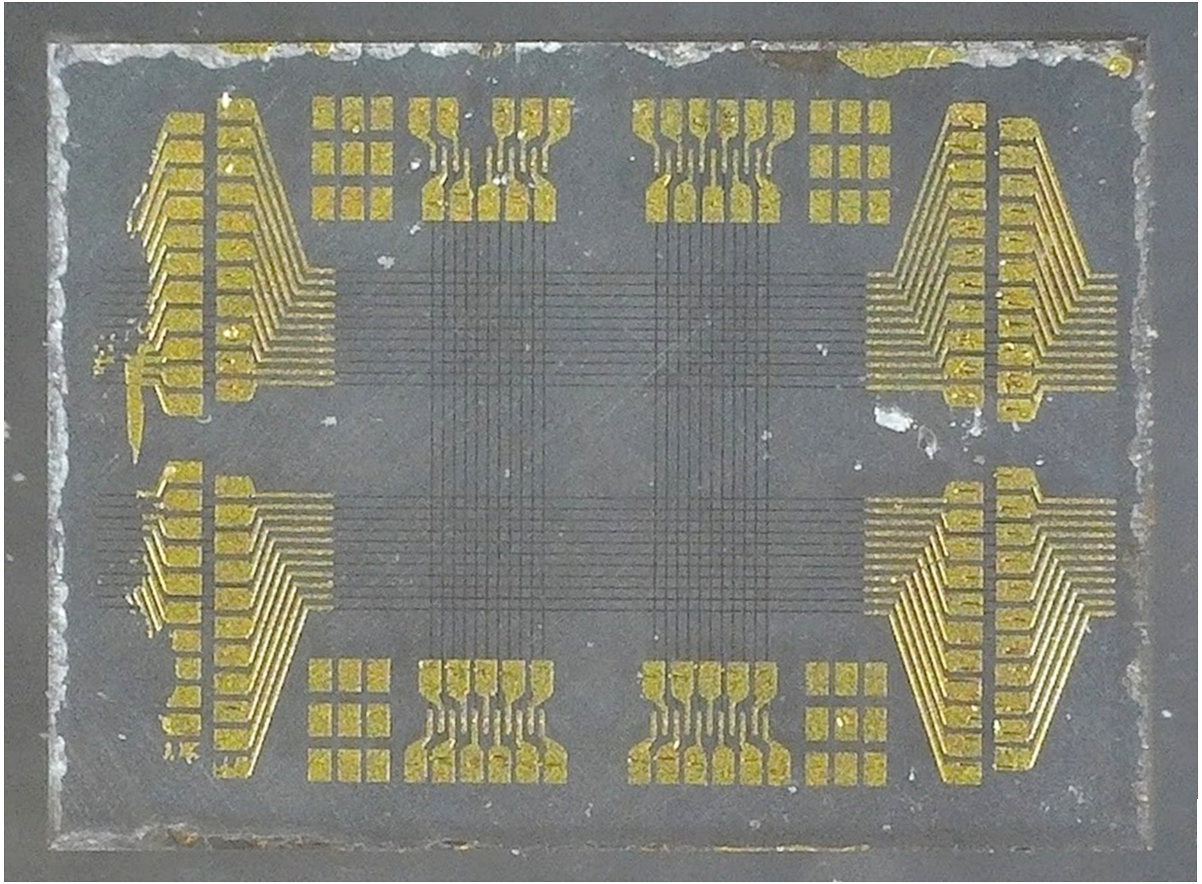

Fabrication

Wire bonding:
Frank Courtney
(U. Warwick)

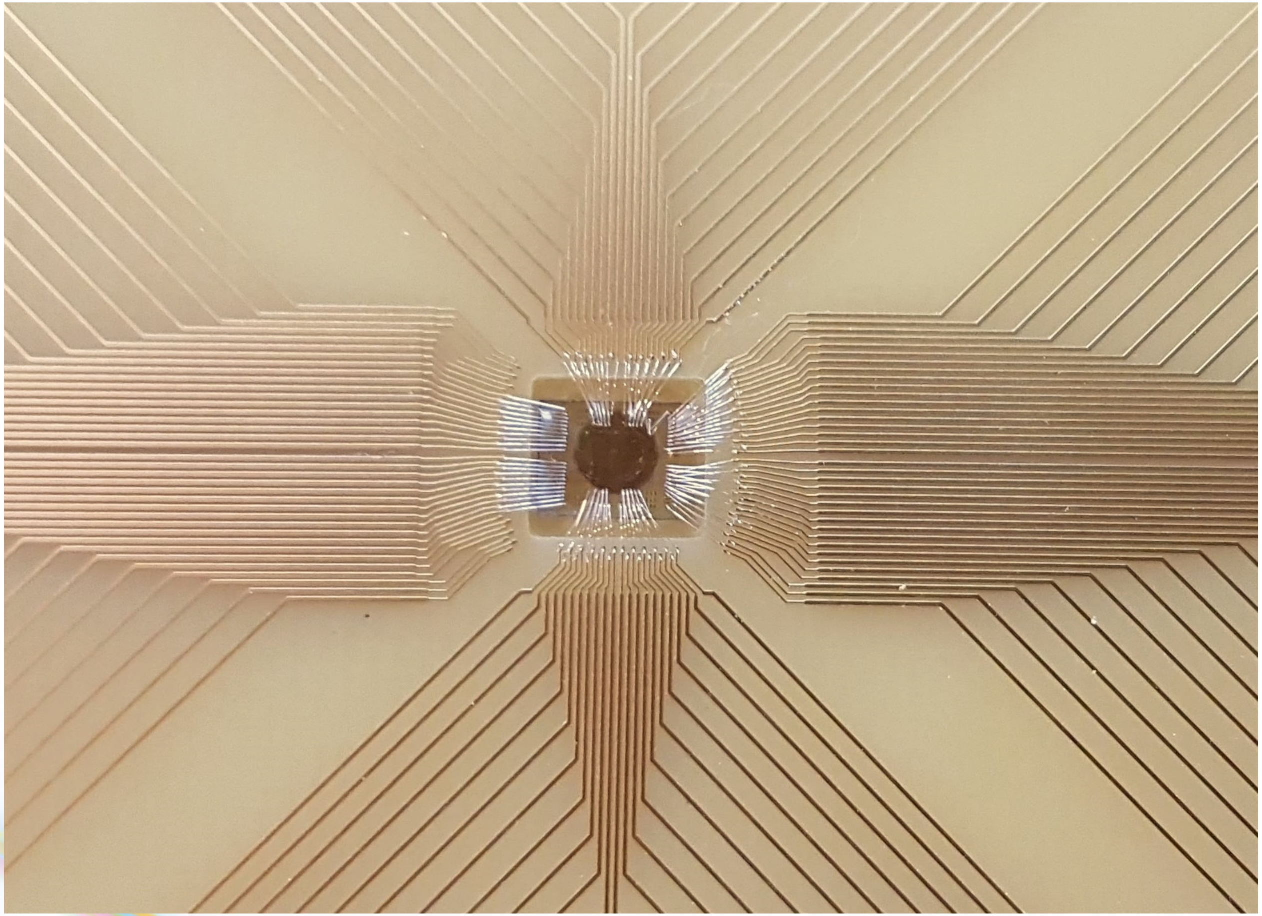

Fabrication

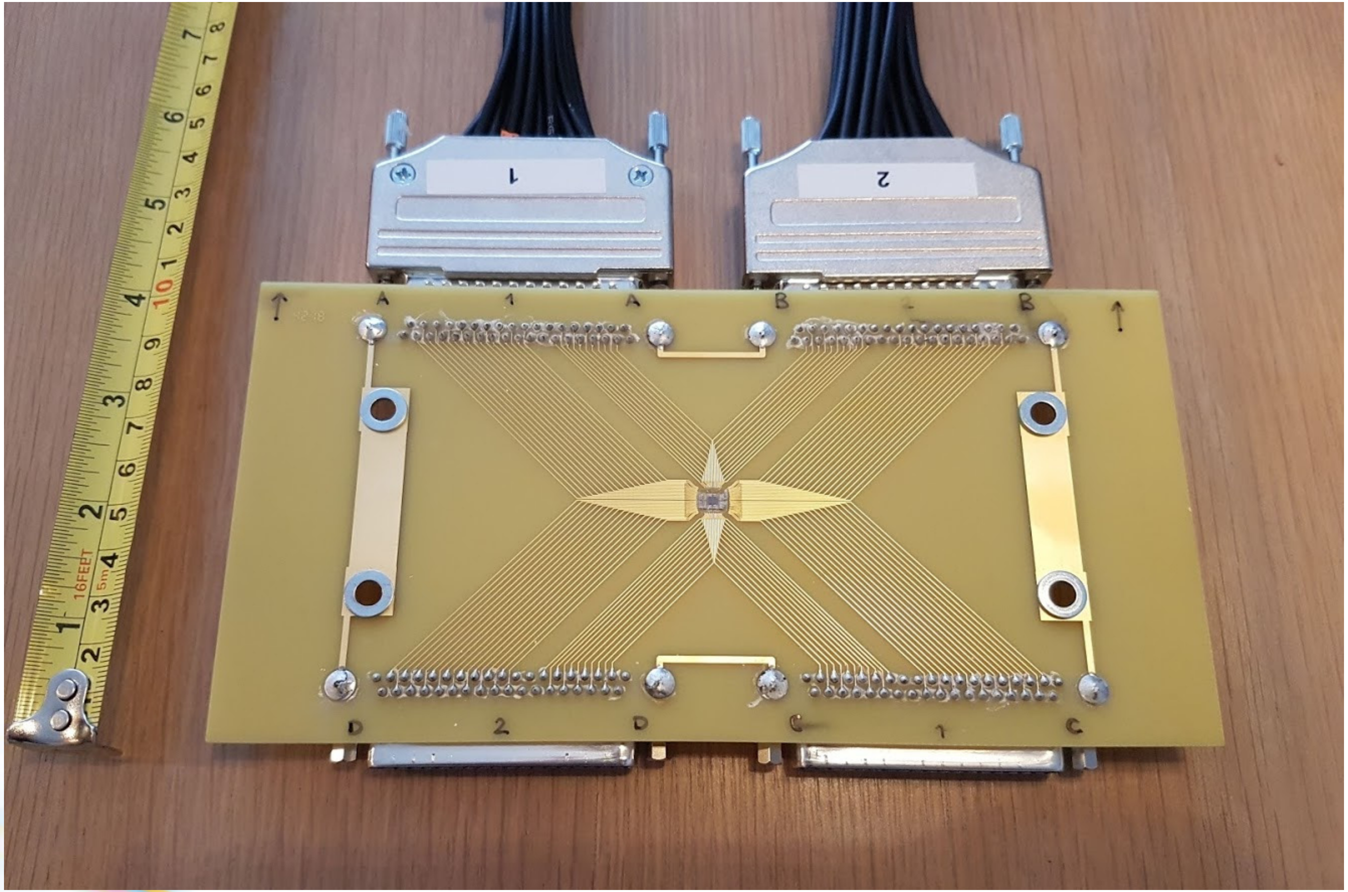

Experimental set-up

Experimental set-up on
Diamond's **I18** beamline:

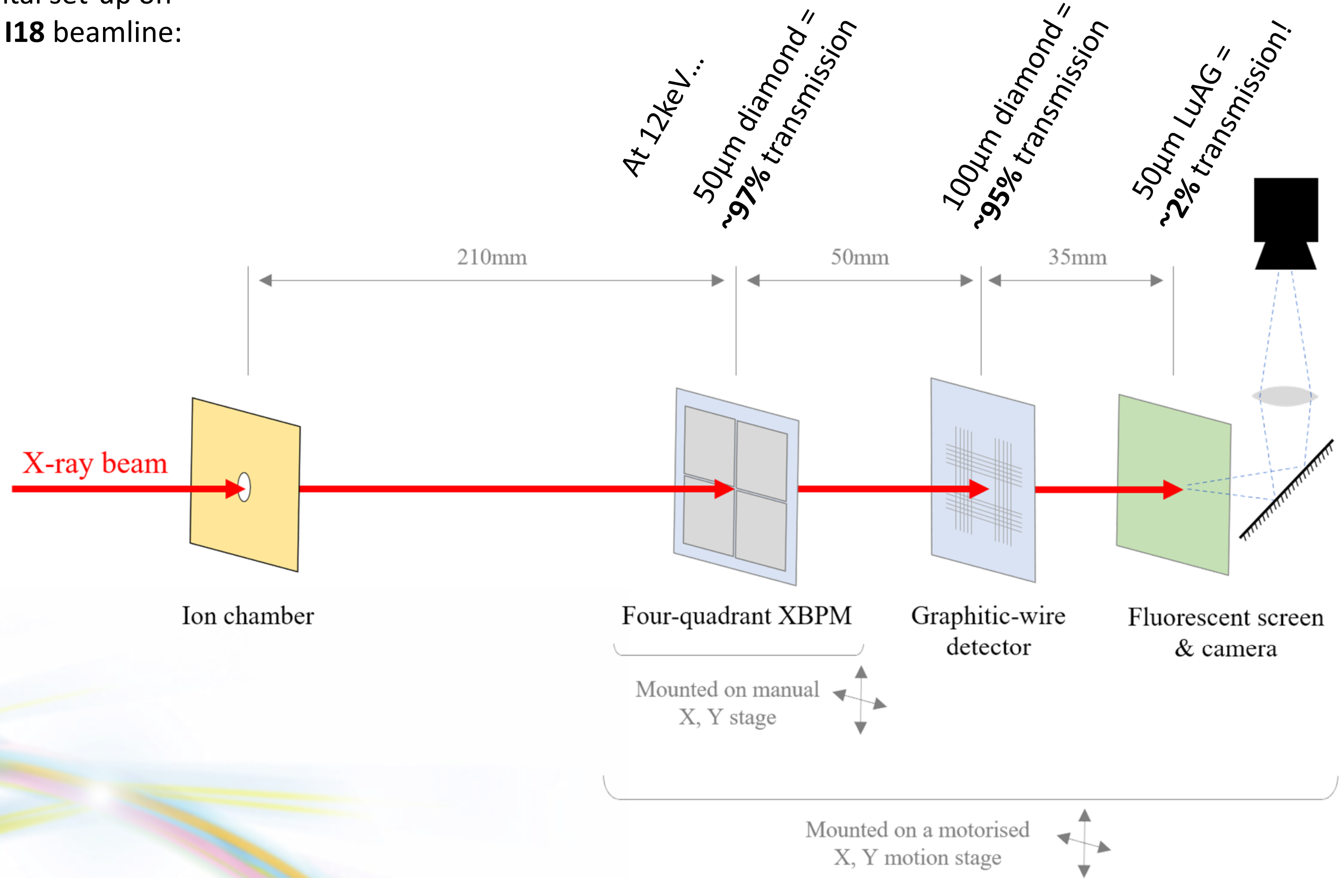

Experimental set-up

Experimental set-up on
Diamond's **I18** beamline:

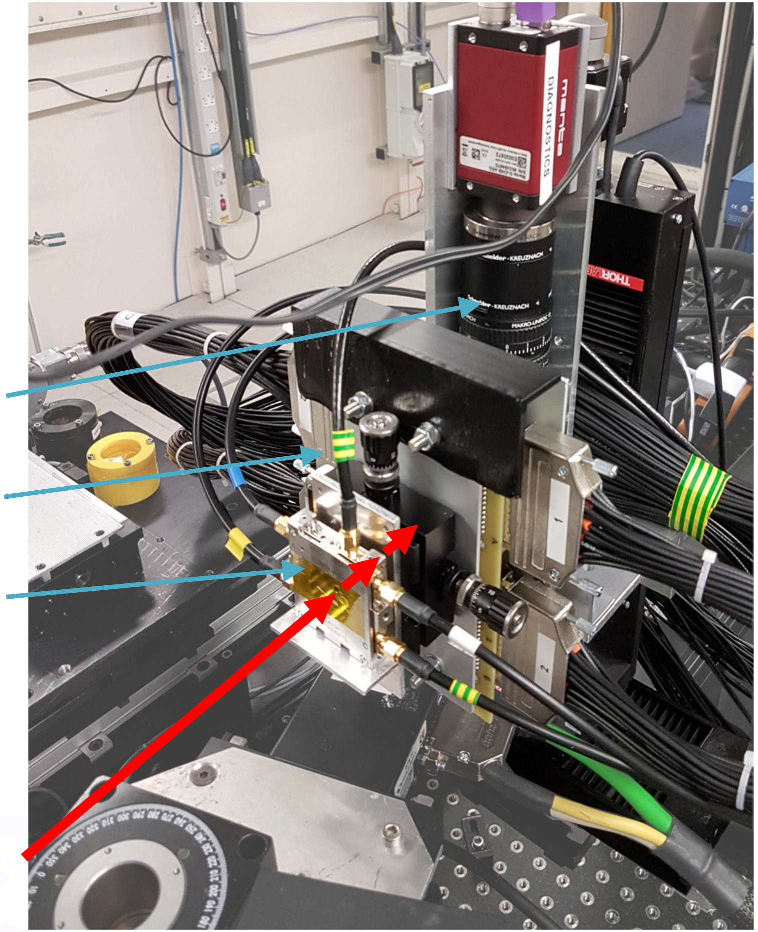

Fluorescent screen & camera

Graphitic wire detector

Four-quadrant XBPM

Results

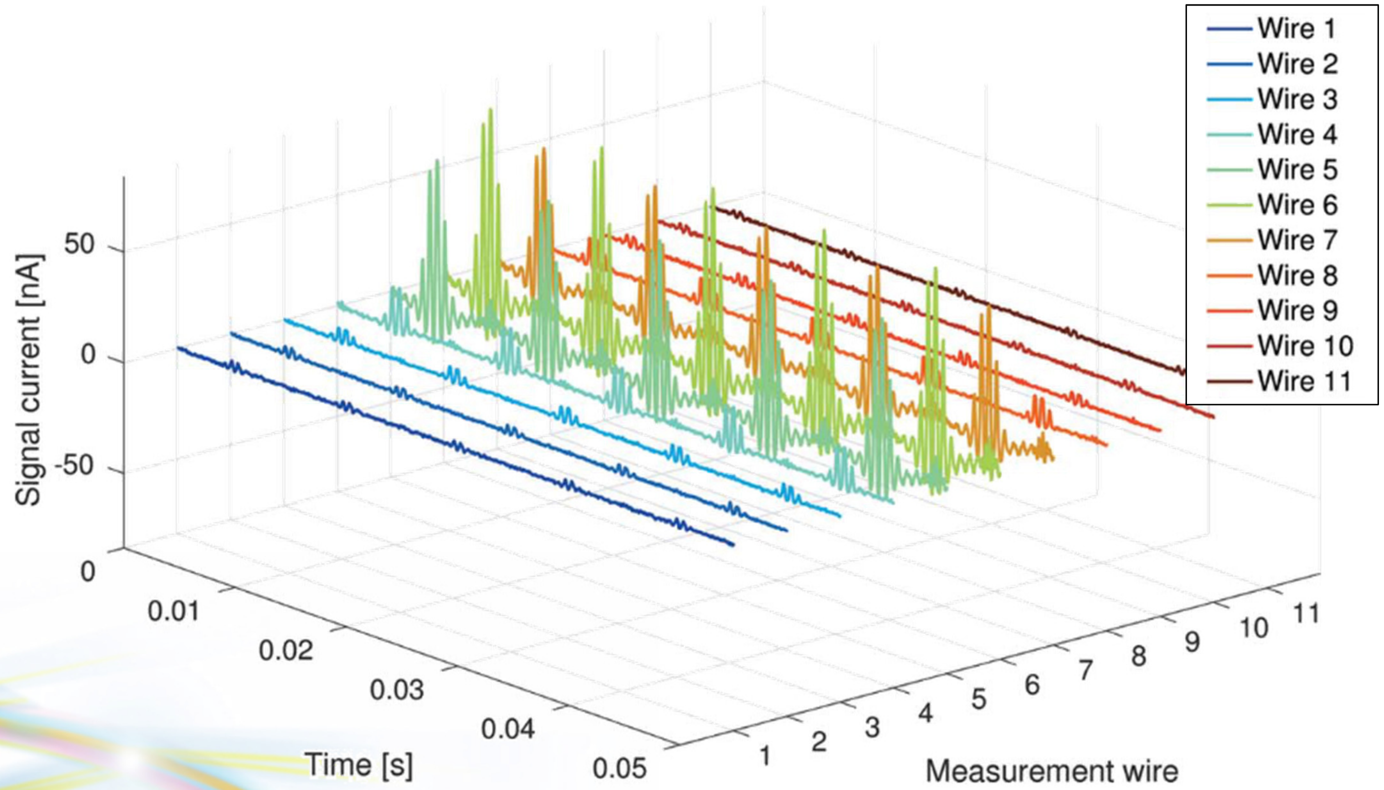
Signal current [nA]
50
0
-50
0
0.01
0.02
0.03
0.04
0.05
Time [s]
1
2
3
4
5
6
7
8
9
10
11
Measurement wire
Wire 1
Wire 2
Wire 3
Wire 4
Wire 5
Wire 6
Wire 7
Wire 8
Wire 9
Wire 10
Wire 11

Results

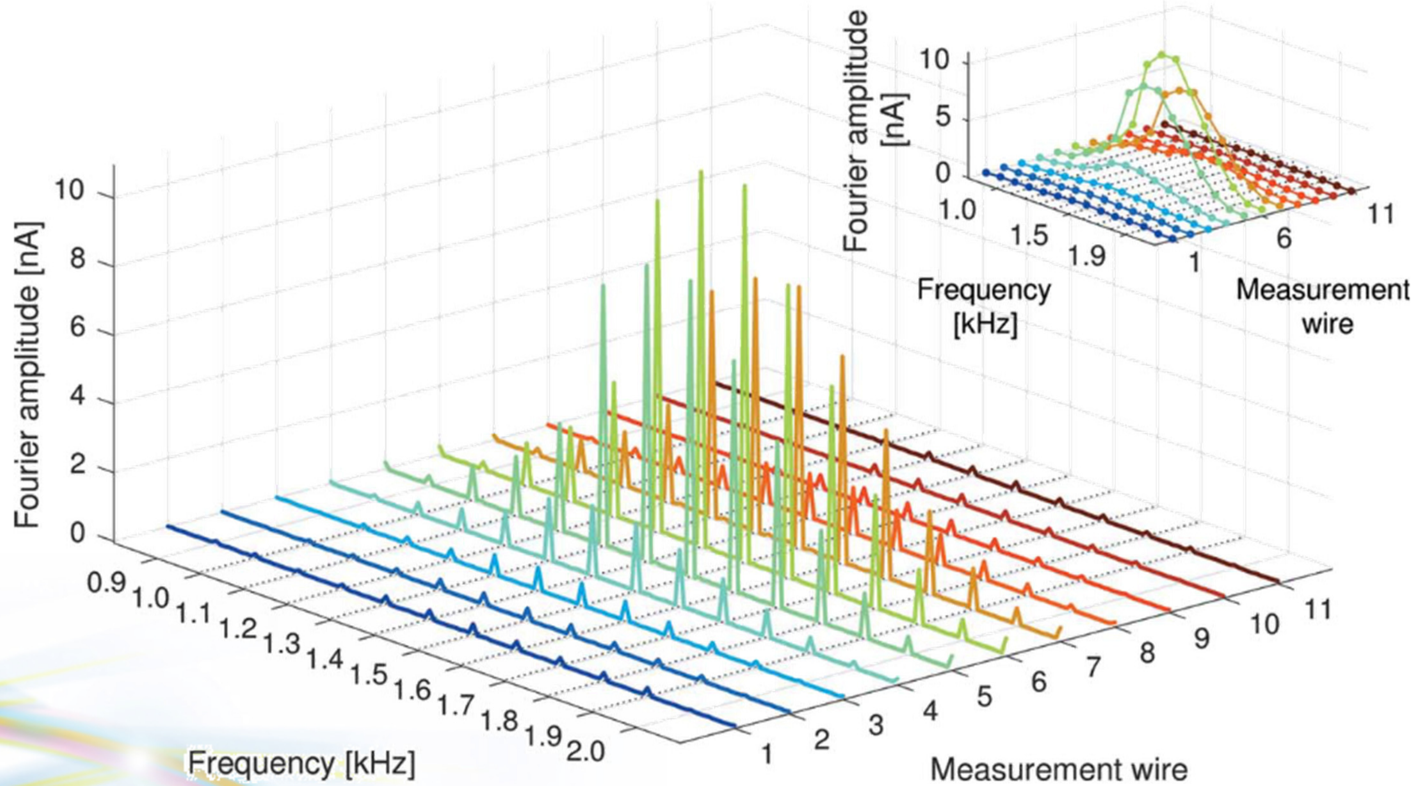
Fourier amplitude [nA]
10
8
6
4
2
0
0.9
1.0
1.1
1.2
1.3
1.4
1.5
1.6
1.7
1.8
1.9
2.0
Frequency [kHz]
1
2
3
4
5
6
7
8
9
10
11
Measurement wire
Fourier amplitude [nA]
10
5
0
1.0
1.5
1.9
Frequency [kHz]
1
6
11
Measurement wire

Results

Illuminating the detector with a 100µm x 70µm photon beam, 10keV.

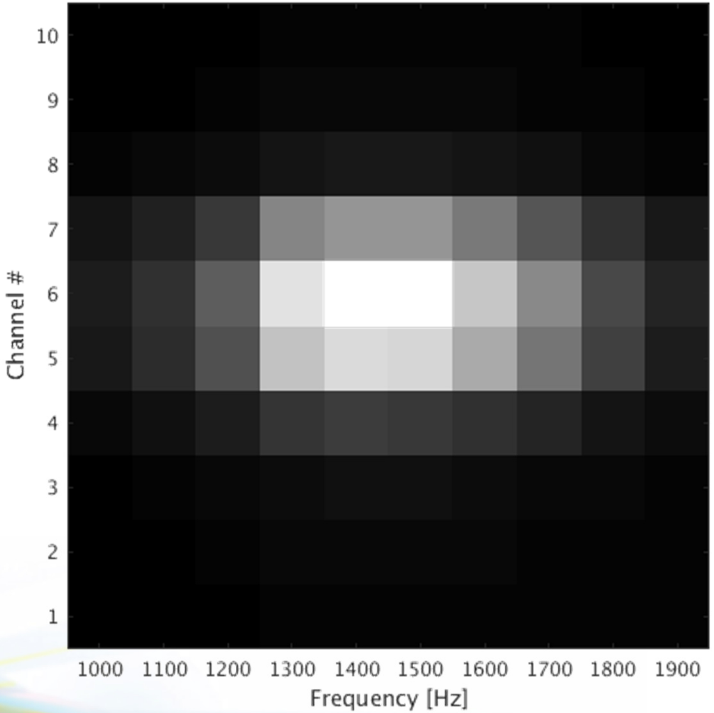

Since distance between wires is known to be exactly 50µm we can directly determine the pixel location.

Results

Illuminating the detector with a 100µm x 70µm photon beam, 10keV.

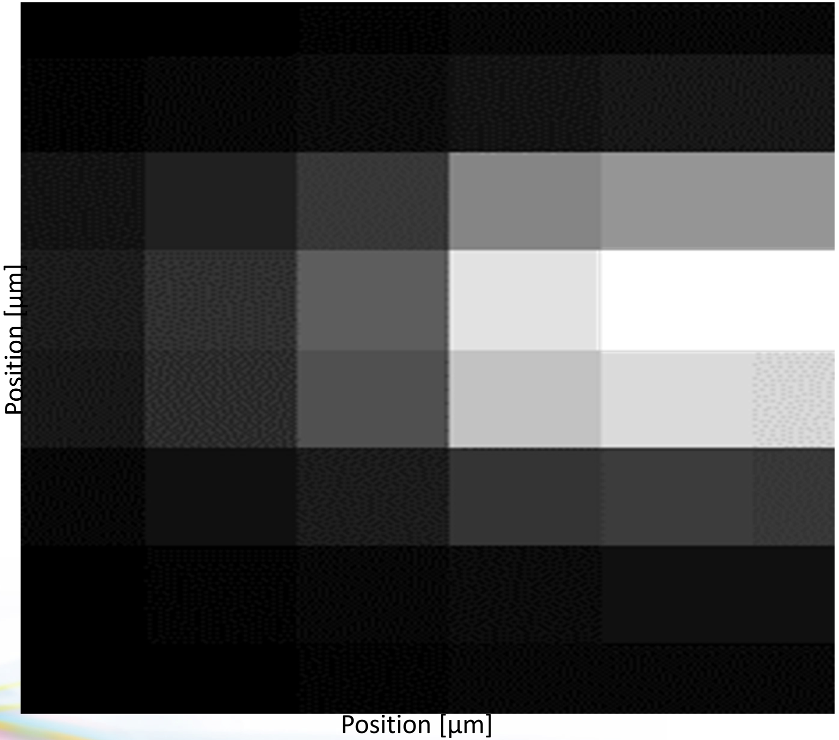

Since distance between wires is known to be exactly 50µm we can directly determine the pixel location.

Results

Illuminating the detector with a 100µm x 70µm photon beam, 10keV.

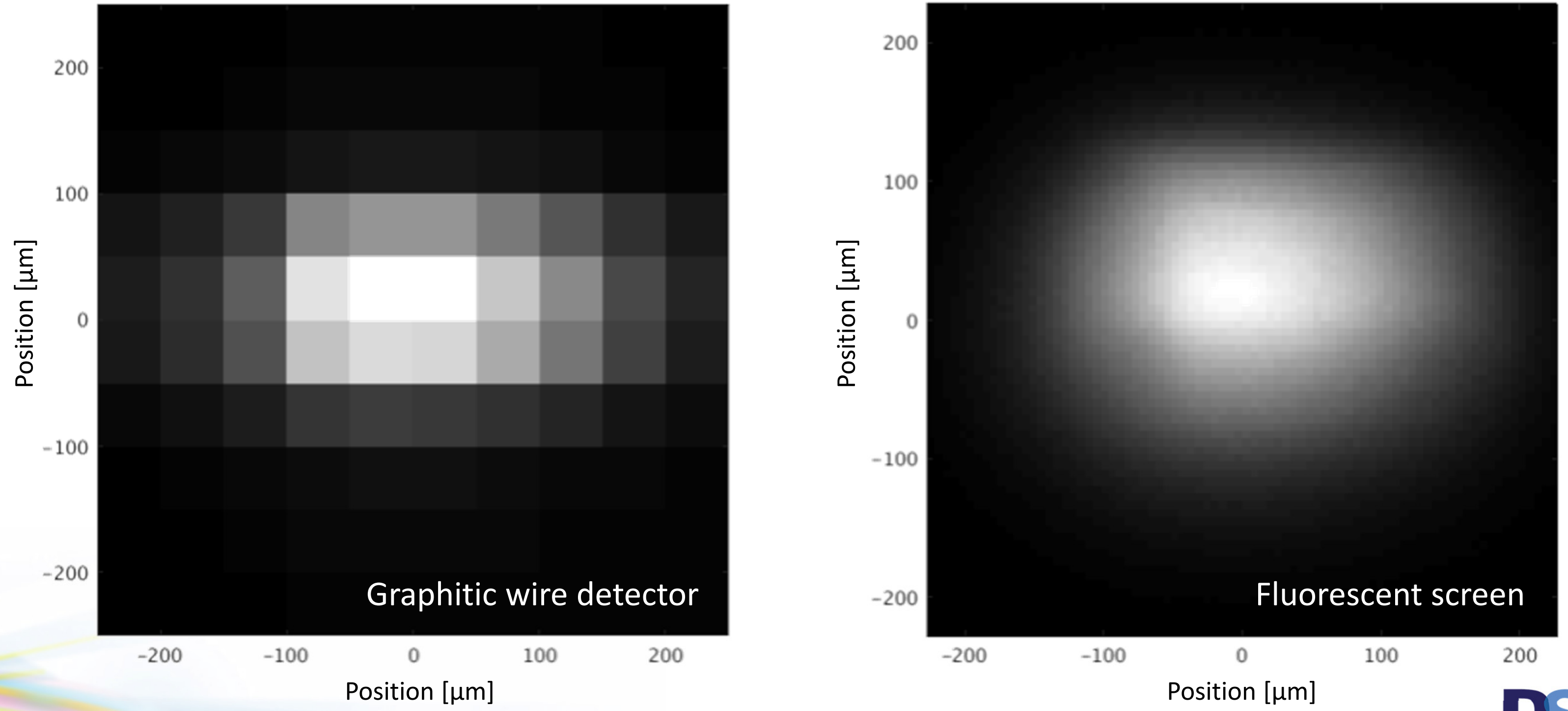

Results

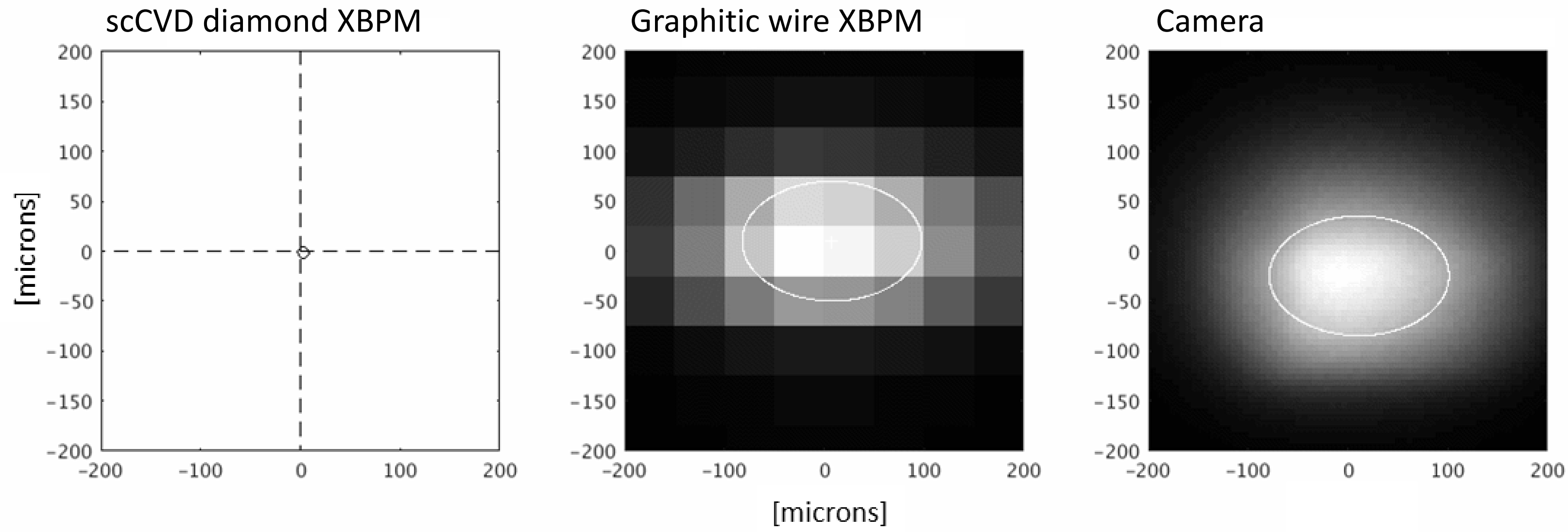
scCVD diamond XBPM

Graphitic wire XBPM

Camera

Results

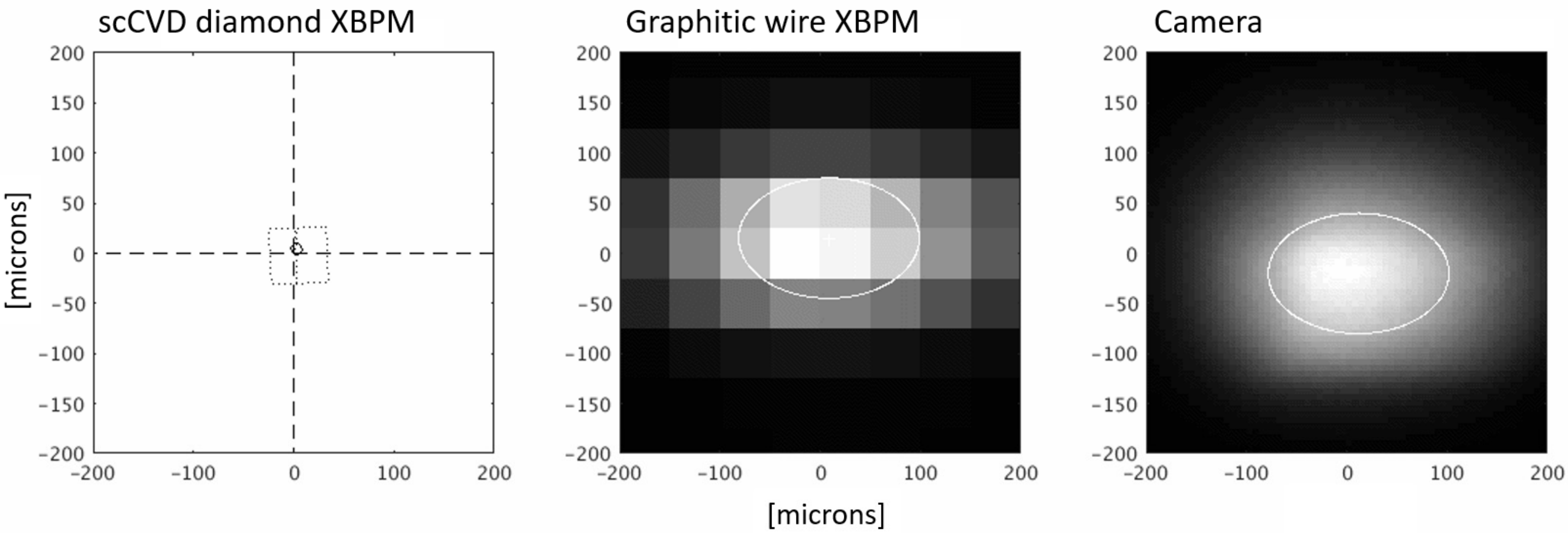
scCVD diamond XBPM
Graphitic wire XBPM
Camera
[microns]
[microns]
200
150
100
50
0
-50
-100
-150
-200
-200
-100
0
100
200

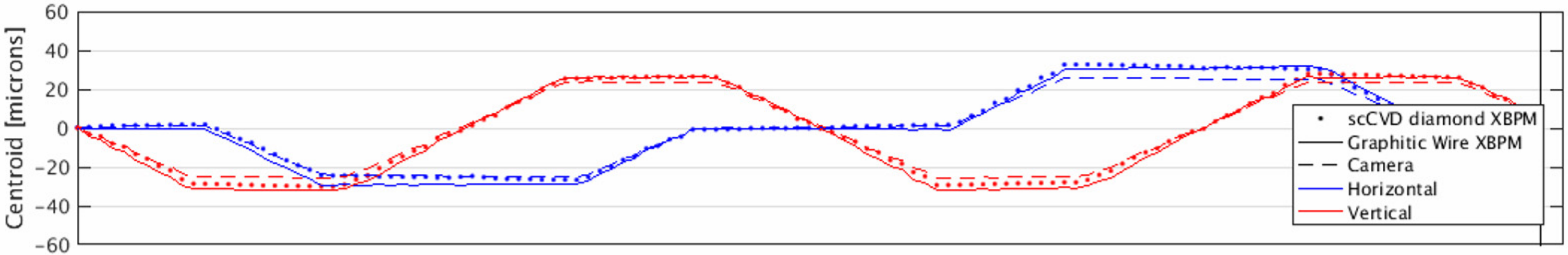
Centroid [microns]
60
40
20
0
-20
-40
-60
• scCVD diamond XBPM
Graphitic Wire XBPM
Camera
Horizontal
Vertical

Results

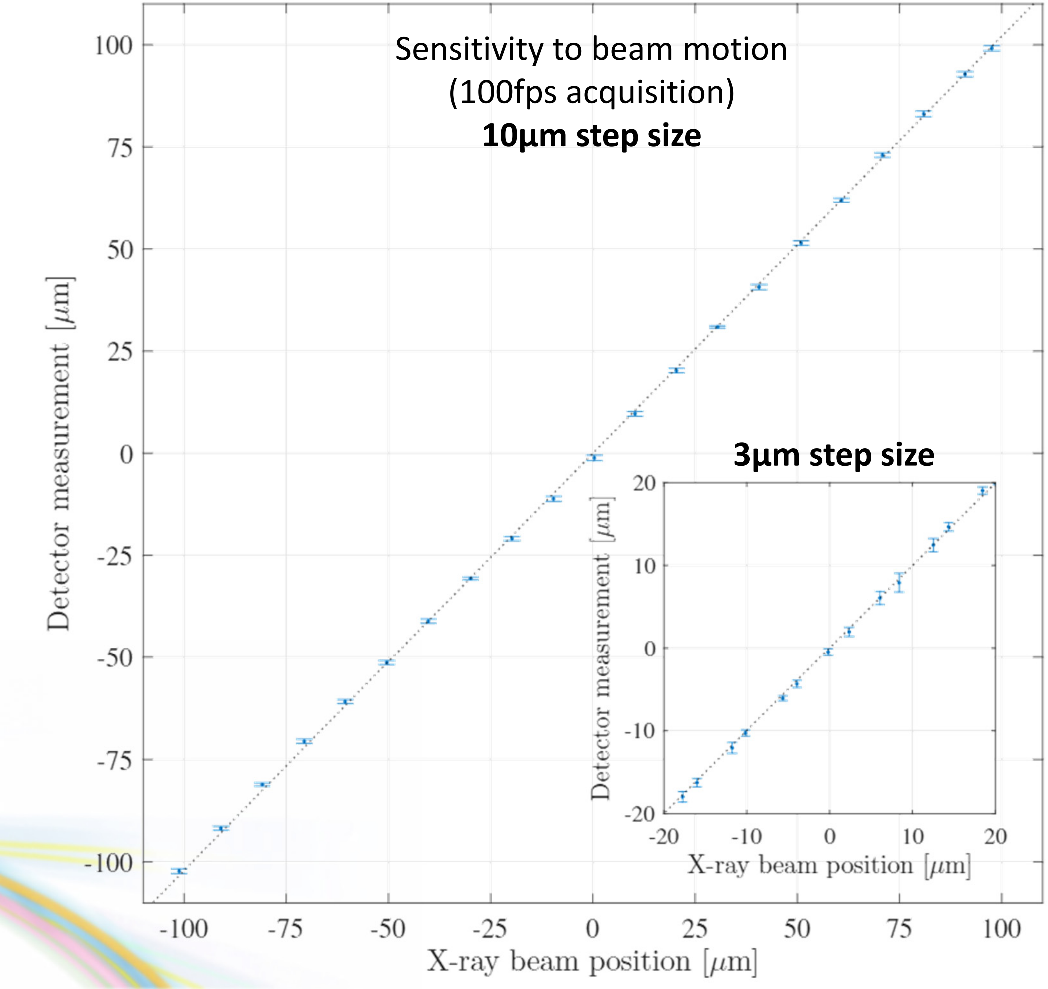

Average of 600nm
r.m.s. noise
(0.3% of beam size)

Results

Position [µm]

Position [µm]

Position [µm]

Results

Estimation of the spread function:

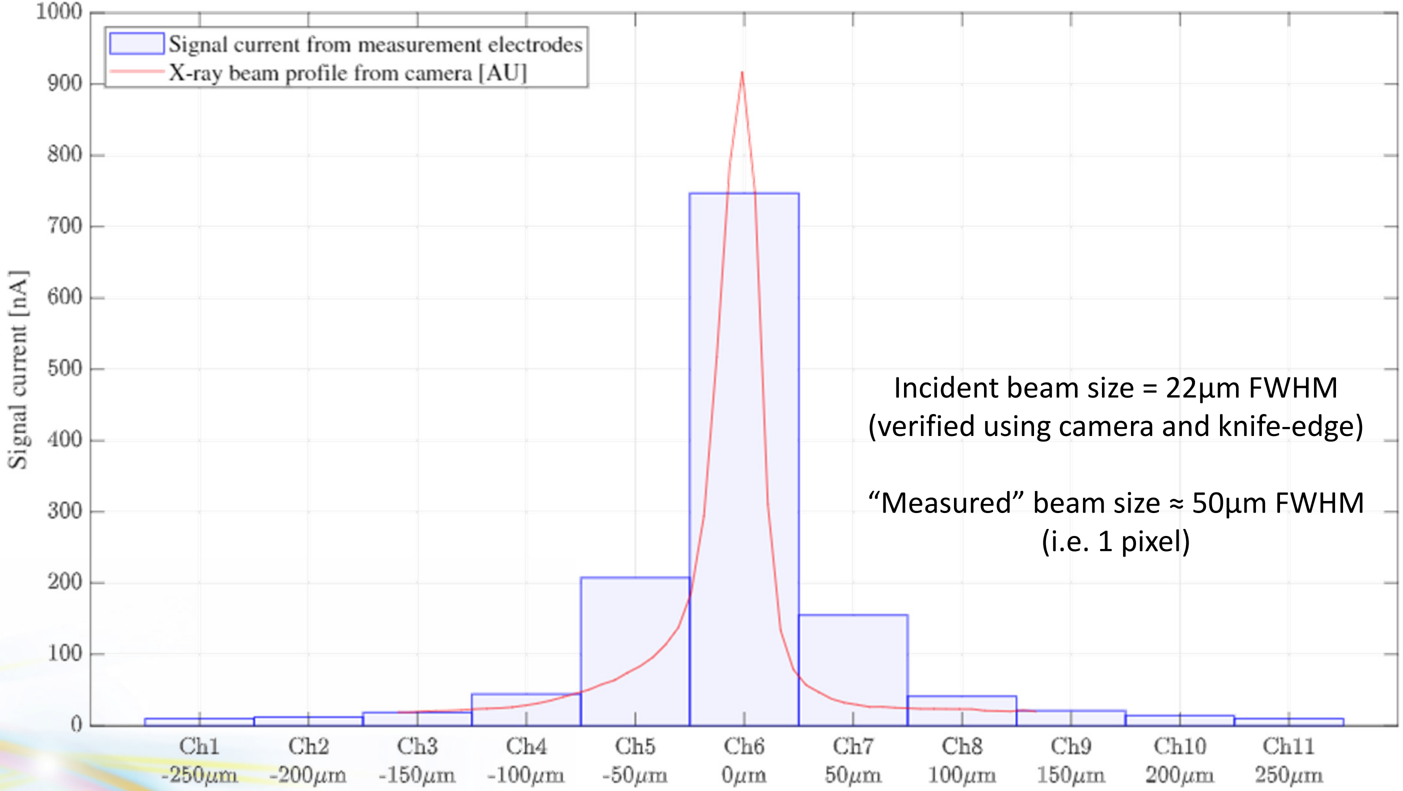

Incident beam size = 22µm FWHM
(verified using camera and knife-edge)

“Measured” beam size ≈ 50µm FWHM
(i.e. 1 pixel)

Future work

Modelling to optimising electrode geometries:
improve charge collection efficiency and reduce lateral charge drift

Diffusion of individual charge carriers is calculated from **Wiener process** (i.e. Brownian motion).
Probability of finding particle at location *x* after **time** *t*:

$$p(t,x) = \frac{1}{\sqrt{4\pi D(t-t_0)}} \exp\left(-\frac{(x-x_0)^2}{4D(t-t_0)}\right) \qquad (1)$$

Net drift velocity determined by **mobility**, *μ*, and **field** *E*.
However, limited by **saturation velocity** v_s:

$$\vec{v_e} = \frac{\mu_e \vec{E}}{1 + \frac{\mu_e \vec{E}}{v_{e,s}}} \quad , \qquad \vec{v_h} = \frac{\mu_h \vec{E}}{1 + \frac{\mu_h \vec{E}}{v_{h,s}}}$$

i.e. change in **position** after **time**, *t*:

$$\vec{x_e}(t) = \vec{v_e}\ t \quad , \qquad \vec{x_h}(t) = \vec{v_h}\ t \qquad (2)$$

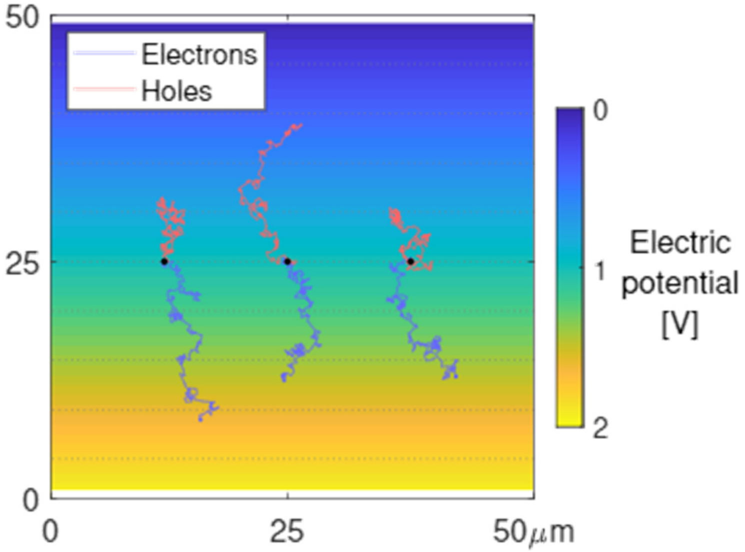

Future work

Modelling to optimising electrode geometries:
improve charge collection efficiency and reduce lateral charge drift

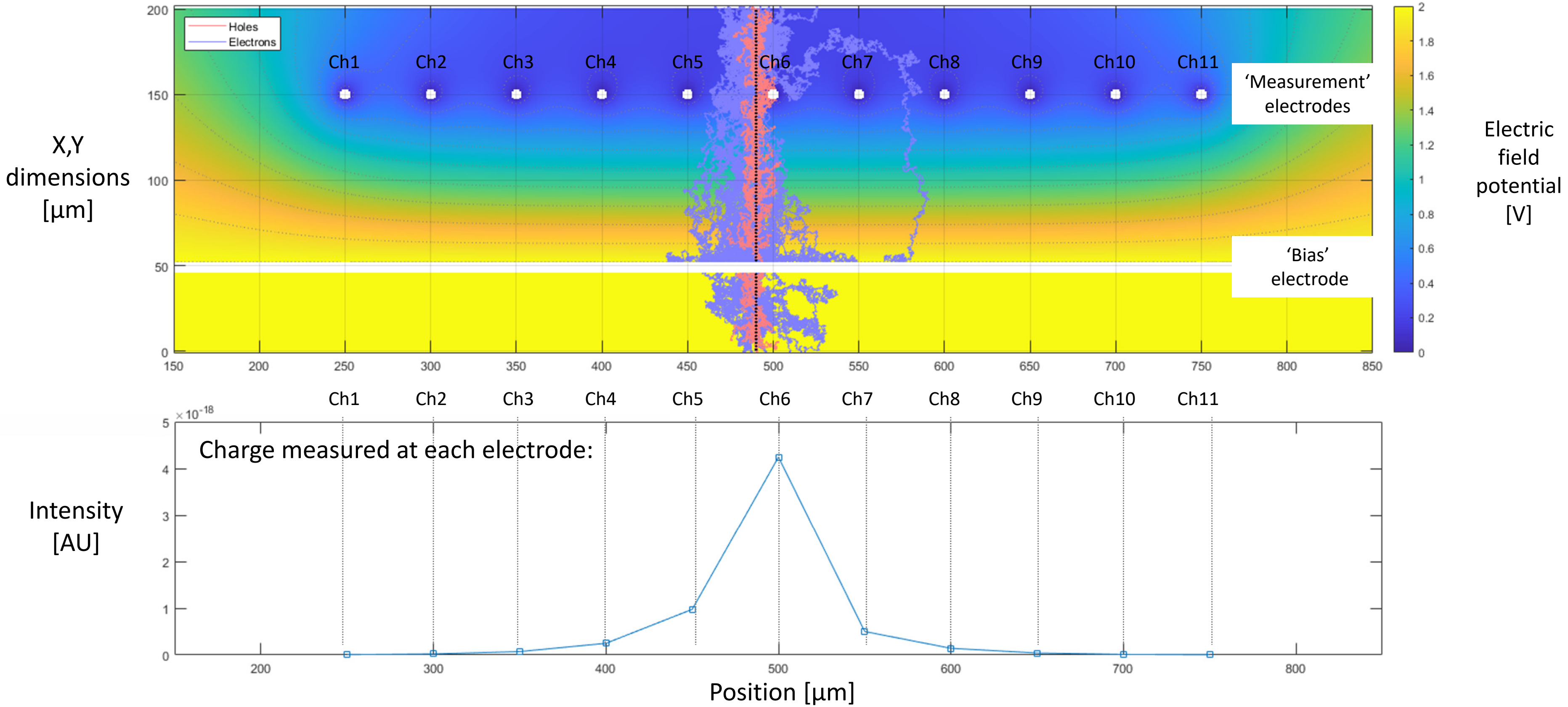

Acknowledgements

University of Warwick
Ben Green
Frank Courtney
Yash Lekhai
Yorck Ramachers

Element Six
Andy Edmonds

Diamond Light Source
Graham Cook
Steve Keylock
Ben Bradnick
Konstantin Ignatyev
Guenther Rehm

Conclusions

- We successfully built an imaging detector with graphitic electrodes buried under the diamond surface and obtained synchrotron X-ray beam profile measurements.
- Within the instrument's transmissive aperture there is no surface metallisation that could absorb X-rays, and no surface structures that could be damaged by exposure to synchrotron radiation beams.
- The simultaneous read out of all pixels at 100fps has been achieved using a novel lock-in technique.
- Intensity measurements of up to 0.5% of mean intensity, and position measurement of up to 0.3% of beam size have been demonstrated.
- Future work will concentrate on improving pixel count, and improving charge collection efficiency.